Raman Spectroscopy of Benzenethiolates on Nanometer-Scale Gold Clusters†

Ryan C. Price and Robert L. Whetten*

Department of Chemistry and Biochemistry, Georgia Institute of Technology, Atlanta, Georgia 30332

Received: May 9, 2006; In Final Form: September 20, 2006

Near-infrared (1064-nm) irradiation of neat solid samples of benzenethiolate monolayer-protected gold clusters (MPCs) yields strong, well-resolved Raman spectra of the thiolate groups, comparable to those obtained for the same groups adsorbed at roughened gold electrodes. These clusters are formulated as $TOA_Z[Au_N(SPh)_M]^{Z-}$, $N \gg M$ and $Z = 3-6$, with core diameters of 1.7 and 1.5 nm, and were characterized previously by X-ray scattering, mass spectrometry, infrared spectroscopy, optical spectroscopy, nuclear magnetic resonance, and elemental analysis [Price, R. C.; Whetten, R. L. *J. Am. Chem. Soc.* **2005**]. Numerous previous attempts to obtain spectra on various MPCs yielded only diffuse luminescence bands, as did benzenethiolate MPC samples of $TOA_2[Au_{44}(SPh)_{28}]^{2-}$, with 1.1-nm core diameters. The clusters are free of excess tetraoctylammonium bromide (TOABr) from the synthetic procedure, containing only the necessary TOA^+ to maintain charge balance. In situ thermometry, using the anti-Stokes/Stokes intensity ratios, indicated the sample temperature remained below the onset of thermal decomposition. The Raman spectra of the clusters bear a strong resemblance to those obtained for nonmetallic $(Au^{(I)}SPh)_x$ polymer samples that are not in resonant absorption at the laser wavelength. The smaller of the two cores, nominally $TOA_6[Au_{110}(SPh)_{62}]$, shows clearly a band at 505 cm^{-1} assigned to a S−S stretch, suggestive of a moiety resembling diphenyl disulfide on the cluster surface. These results are interpreted with reference to recent reports suggesting a substantial "reconstruction" of the outermost gold layer upon thiolate adsorption (SAM formation).

Introduction

Raman scattering by thiolate monolayers on noble metal bulk and colloidal surfaces has been intensively studied for the information it provides on the structure and bonding of the adsorbate groups.[1−3] We have recently applied this method to large gold clusters with core diameters of 1.7 and 1.5 nm containing fewer than 150 gold atoms. In a previous report, the compositions of these simultaneously generated, readily separable monolayer protected clusters (MPCs) have been nominally formulated as $\sim TOA_3[Au_{140}(SPh)_{78}]$ and $\sim TOA_6[Au_{110}(SPh)_{62}]$, where TOA is the tetraoctylammonium counterion.[4] The Raman spectra of these materials share many features with a polymeric $Au^{(I)}SPh$ sample, much like earlier reports of benzenethiolate (−SPh) and diphenyl disulfide (DPDS) on roughened gold electrodes.[5−7] This work provides a better understanding of benzenethiolate binding on small gold MPCs, but a complete understanding of the gold thiolate interaction remains elusive.

The nature of the bonding in gold−thiolate monolayers on extended crystalline surfaces is not fully understood, but disulfide species are generally not detected, with the exception of 4-pyridinethiolate on Au(111).[8] Surface spectroscopic measurements of benzenethiolate self-assembled monolayers (SAMs) have determined a 76° tilt angle from the surface normal for the aromatic ring.[7] Initial reports on the lateral ordering of benzenethiolate on Au(111) found no ordered phases,[9,10] but more recent work by Osawa et al. found a nearly$(\sqrt{13} \times \sqrt{13})R13.9°$ monolayer symmetry and a ∼30° ring tilt angle from the surface normal in aqueous solution utilizing surface enhanced infrared absorption spectroscopy and scanning tunneling microscopy.[11] Infrared spectra we obtained on the clusters and $(Au^{I}SPh)_x$ polymer did not reveal any additional insights into the nature of benzenethiolate on the surface of the MPCs, but are included in the Supporting Information for completeness. It seems likely that solvent and thiol concentration during benzenethiol chemisorption at *crystalline* surfaces may determine the characteristics of the monolayer formed and could differ greatly from benzenethiolates on small clusters formed via the complete reductive degradation of a $[Au^{(I)}/thiolate]_x$ polymer.[12] In contrast to the earlier assumptions (implicit or explicit) that the structure of the outermost metal layer is unmodified by SAM formation, several recent experimental and theoretical reports assert a substantial reconstruction of noble metal surfaces by bound thiolates.[13a−h] This phenomenon could alter the electronic density of states of metal/thiolate MPCs and explain the unusually high optical-absorbance onset energies reported for $Au_{38-44}(arylthiolate)_{24-28}$ MPCs.[4,14] Unusually high symmetry within these clusters could also yield high band gaps, as found for the "unprotected" tetrahedral Au_{20} cluster.[15]

The goal of this study was to obtain the Raman spectra of discrete, molecular-scale $Au_N(SPh)_M$ MPCs for comparison to earlier reports of −SPh on gold extended surfaces to better understand the binding of thiolates on small gold cores and the role surface monolayer may have on cluster properties. The spectral similarities strongly suggest that the binding modes are similar to those of extended SAMs with low coordination numbers (i.e., 1:1 Au/S), which are also characteristic of $(Au^{(I)}SPh)_x$ polymer phases. The presence of polymeric surface phases cannot be ruled out for gold MPCs and will play a large role in determining the properties of these materials if present.

Experimental Section

The two-step preparation and purification of the $Au_N(SPh)_M$ MPCs with core diameters of ∼1.5 and 1.7 nm are detailed

† Part of the special issue "Charles M. Knobler Festschrift".

* E-mail: whetten@chemistry.gatech.edu.

10.1021/jp062840r CCC: $33.50
Published on Web 10/04/2006

elsewhere.[4] Briefly, 20 mL of 75 mM aqueous $HAuCl_4$ is added to 75 mL of dichloromethane that is 24 mM in tetraoctylammonium bromide and 60 mM in benzenethiol. Vigorous stirring for 16 h ensures Au/SPh/TOA complex formation. Next, 20 mL of 750 mM $NaBH_4$ is rapidly added and stirred 24 h to ensure complete reduction. The molar ratios of Au/thiol/TOABr/$NaBH_4$ are 1:3:1.2:10, respectively. The resultant MPC solution is dried by rotary evaporation to remove the majority of the dichloromethane, precipitated thrice with ethanol (150 mL each), transferred onto a 0.16-μm filter with acetonitrile, and rinsed twice with acetonitrile (80 mL) to remove residual TOABr. Elution with ~100 mL of toluene yields 1.5-nm clusters, followed by dichloromethane elution to yield 1.7-nm clusters. Each eluted fraction is easily dried to produce nanocrystalline powders.

The 1.1-nm $TOA_2[Au_{44}(SPh)_{28}]$ clusters are prepared from the 1.5-nm ~$TOA_6[Au_{110}(SPh)_{62}]$ MPCs via an oxidative etching process as follows. In pure tetrahydrofuran (15 mL) are dispersed 1.5-nm core clusters (31.9 mg, ~118 μmol Au) with continuous stirring. Benzenethiol (12 μL, 118 μmol) and 30% aqueous hydrogen peroxide (120 μL, 1.18 mmol) are added. The reaction completes within 3 h, indicated by a complete color change from dark brown to pale olive and readily verifiable by optical spectroscopy. The solution is dried by rotary evaporation, and the MPCs are transferred to a 0.16-μm syringeless filter with acetonitrile and rinsed thrice with acetonitrile (50 mL) to remove byproducts. Acetone (80 mL) is injected through the syringeless filter to remove any residual diphenyl disulfide. The solids are then eluted with toluene (50 mL), yielding 12.0 mg of 1.1-nm MPCs. They are soluble at 400 μM in dichloromethane and 700 μM in toluene. The product yield with respect to gold is 34%.

The preparation of the $(Au/SPh)_x$ polymer[16] is as follows: A 3:1 molar ratio of benzenethiol (Aldrich) is combined with $HAuCl_4$ in methanol and stirred until a white precipitate results, in accordance with the stoichiometric reaction: $3PhSH + HAuCl_4 \rightarrow (Au^{I}SPh) + PhSSPh + 4HCl$. This solution is then dried by rotary evaporation and rinsed with copious amounts of acetone to remove excess diphenyl disulfide, followed by drying to yield $(Au/SPh)_x$ as an insoluble white powder. Sodium benzenethiolate (NaSPh) and diphenyl disulfide (DPDS) were purchased from Aldrich and used without further purification.

Approximately 2−3 mg of each dry, free-flowing sample were manually pressed with a steel rod into a pellet within a stainless steel target/sample holder. Each sample was placed in a Bruker FRA 106/S FT Raman Module attached to a Bruker Equinox 55 FTIR spectrometer. The instrument has a fixed path length and focal length. The excitation for Raman scattering is at 1064 nm (9399 cm^{-1}, 1.165 eV) with a typical fluence of 75 mW. The laser focus area is ~0.80 mm^2, and spectra were typically collected at ~94 W/m^2 for 16 or 32 scans at 2 cm^{-1} resolution through the spectral range ~600−3200 cm^{-1} in a duration of about two minutes. The notch filter inhibiting Rayleigh radiation detection occluded ±150 cm^{-1}, precluding detection of Au−Au modes.

The spectra were reproducible over time and for different synthetic batches of the same material. Independent evaluation of the 1.7-nm clusters with a Thermo Nicolet NXR FT-Raman spectrometer at an excitation wavelength of 1064 nm with a null filter (0.3 mW, 640 scans) produced the same spectrum with a superior signal-to-noise ratio compared to our data.[17] Larger numbers of scans and higher fluences tended to degrade the samples to bulk gold, providing spectra devoid of benzenethiolate features. Anti-Stokes shifts were utilized to estimate sample temperatures and compared with thermogravimetric data for the materials, verifying sample stability during data collection.

Results and Discussion

The Raman spectra for $Au_N(SPh)_M$ MPCs resemble $(Au/SPh)_x$ polymer species, similar to previous observations for benzenethiol, diphenyl disulfide (DPDS), and phenyl sulfide chemisorbed on bulk gold.[5−7] Spectra for the clusters and the $Au^{(I)}SPh$ polymer, shown in Figure 1, all display similar relative intensity enhancement of vibrations at 1582 cm^{-1} (a_1), 1070 cm^{-1} (b_2), and 416 cm^{-1} (a_1), relative to the 999 cm^{-1} a_1 mode (see Supporting Information for modes). There are several noteworthy spectral features, the most prominent being the appearance of a cis-oriented diphenyl disulfide S−S stretch in the 1.5-nm $Au_N(SPh)_M$ cluster spectrum at 507 cm^{-1}. Splitting and shifting of the diphenyl disulfide S−S stretch at 542−515 cm^{-1} (trans) and 505 cm^{-1} (cis) have been assigned previously for DPDS in the solid state on Ag(0).[5] The next feature of interest is the softening of the ~1570 cm^{-1} a_1 mode to 1559 cm^{-1}, possibly arising from orientation of the aromatic ring closer to the gold surface, as reported for benzenethiolate on iron and platinum.[18,19] Last, no evidence of Au−Cl vibrations at 324 or 347 cm^{-1} or Au−Br vibrations at 202 or 212 cm^{-1} are observed in the $Au_N(SPh)_M$ MPCs, indicating no gold−halide bonds to induce a metal to insulator transition, such as those observed in $Au_{55}(PPh_3)_{12}Cl_6$.[20a,b]

While the goal of this study is not to quantify surface enhancement Raman effects, it is significant that the 1070 cm^{-1} b_2 mode is 8−34× more intense than the 997 cm^{-1} a_1 mode within the clusters and polymer relative to NaSPh, implying that a metallic surface may not be needed for "selective" enhancement of certain vibrational modes. Raman shifts and relative intensities for the molecules studied are shown in Table 1 to provide relative band intensity ratios within each sample, but not absolute comparisons between spectra. The Raman shifts and their intensities for benzenethiolate on the gold MPCs are quite similar to prior reports for benzenethiol and diphenyl disulfide chemisorbed onto bulk gold surfaces.[5−7]

A broad luminescence rather than a Raman spectrum was obtained under the experimental conditions herein for the smallest 1.1-nm core $TOA_2[Au_{44}(SPh)_{28}]$ MPC[4] and is shown in the Supporting Information. The absence of benzenethiolate Raman scattering features for this MPC likely results from a significantly enhanced luminescence within this cluster relative to larger clusters. In fact, there are numerous reports of broad near-infrared photoluminescence over the spectral range 0.75−1.9 eV for 0.9−1.9-nm gold MPCs protected by a variety of nonaromatic thiolates, and Raman spectra of these surface species remain unreported or undetected.[21a−g] A photoluminescence quantum efficiency of 0.012 for 1.1-nm ~$Au_{38}(SCH_2CH_2Ph)_{24}$ MPCs has been reported, whereas values between ~4.4×10^{-5} and 1.8×10^{-4} are observed for 1.7-nm ~$Au_{140}(S\text{-alkyl})_{53}$ MPCs.[21a,g] Thus, photoluminescence processes for 1.1-nm clusters are approximately 100 times more probable than in clusters, which potentially obscures benzenethiolate Raman scattering with its characteristic quantum efficiency of only ~10^{-7}. The net effect of these quantum efficiencies makes luminescence for 1.1-nm clusters 12×10^3 times more probable than Raman scattering, but photoluminescence would only be 44 to 180 times more likely in 1.7-nm clusters.

In this study, the aromatic samples were irradiated at 1.165 eV (1064 nm), rather than the 1.65−2.41 eV (514−750 nm) previously utilized, and the power per unit area of ~90 ± 20

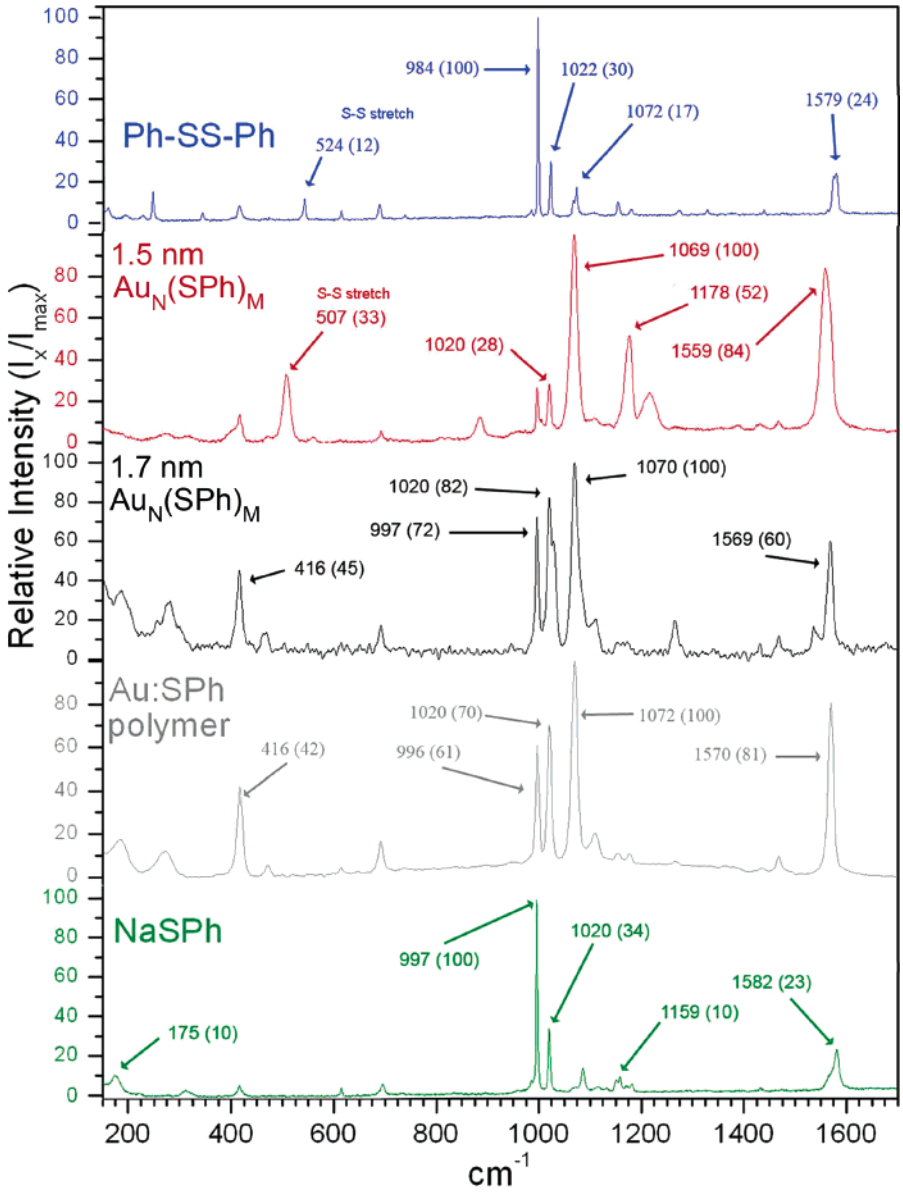

Figure 1. Raman spectra of $Au_N(SPh)_M$ MPCs and reference samples. The five most intense features in each spectrum are labeled with relative intensities in parentheses. Each spectrum is internally normalized with the most intense band assigned as 100%.

W/m^2 was near or below previously reported levels for aromatic thiols on bulk gold,[5−7] but sample degradation from thermal decomposition was initially a concern. Our inability to continuously rotate to refresh the samples during spectrum acquisition and minimize excess heating prompted the estimation of the sample temperatures from the ratios of the relative intensities of the anti-Stokes and Stokes shifts. The relation

$$\frac{I_{AS}}{I_S} \cong e^{-h\Delta\nu/kT} \qquad (1)$$

allows estimation of sample temperature, where I_{AS} and I_S are the relative intensities anti-Stokes and Stokes peaks sharing the same shift, h is Planck's constant, $\Delta\nu$ is the frequency shift (in s^{-1}) of the anti-Stokes/Stokes peak pair, k is the Boltzmann constant, and T is temperature. The estimated temperatures for the clusters are 394 and 315 K for the 1.7- and 1.5-nm cores, respectively. The thermal decomposition onset is at 421 K, indicating sample stability during spectrum collection. The Stokes/anti-Stokes peaks and thermogravimetric data for the 1.7-nm cluster are shown in Figure 2. Both the 1.7- and 1.5-nm cores also displayed a broad luminescence beyond 1700 cm^{-1}, shown in the Supporting Information for completeness. Both the 1.7- and 1.5-nm MPCs absorb strongly in the near-infrared, possessing molar absorption coefficients (ϵ) of approximately 10^5 M^{-1} cm^{-1} at the 1.165 eV Rayleigh line. This suggests the Raman spectra collected may be in resonance. The spectral plots of the $Au_x(SPh)_y$ MPC molar absorptivity coefficients are provided in the Supporting Information.

The benzenethiolate−gold interaction was further probed by ^{1}H NMR spectroscopy, revealing three distinct benzenethiolate moieties for the 1.1-nm $Au_x(SPh)_y$ MPCs[4] that are distributed over a 1.2-ppm spectral range and broad, numerous, less identifiable resonances spanning approximately 2 ppm for the 1.5- and 1.7-nm MPCs. This spectral broadening with increasing cluster diameter has been noted previously for the α and β hydrogens of alkanethiolates and arenethiolates on ≤3.0 nm $Au_x(SR)_y$ MPCs.[23a−e] Both the 1.5- and 1.7-nm $Au_x(SPh)_y$ MPCs possess spectral features resembling the dominant binding modes of the 1.1-nm $[Au_{44}(SPh)_{28}]^{2-}$ clusters, as indicated in Figure 3. This dominant binding mode accounts for 14 of the 28 benzenethiolates of $[Au_{44}(SPh)_{28}]^{2-}$, with the other two minor

TABLE 1: Raman Shifts (in cm^{-1}) with Relative Intensity for Benzenethiolate Species

mode	HSPh[a]	NaSPh	Ph−S−S−Ph	1.5 nm clusters	1.7 nm clusters	$(Au/SPh)_x$
b_1	185	175 {10}	192 {4}	185 {33}	185 {18}	185 {18}
b_2	278		248 {14}	280 {5}	280 {29}	274 {12}
a_1	412	416 {5}		416 {14}	416 {45}	416 {42}
a_2	464			471 {3}	472 {5}	
νS−S			524	507 {33}		
b_2	617	615 {4}	614 {6}			615 {4}
a_1	698	695 {6}	688 {9}	695 {6}	692 {17}	692 {17}
a_1	999	997 {100}	984 {100}	996 {27}	997 {72}	996 {61}
a_1	1023	1020 {34}	1022 {30}	1020 {28}	1020 {82}	1020 {70}
b_2	1072	1072 {4}	1072 {17}	1069 {100}	1070 {100}	1072 {100}
a_1	1093	1086 {14}		1095 {11}		
a_1	1108	1118 {5}	1106 {5}	1108 {12}	1111 {20}	1108 {21}
b_2	1159	1159 {10}	1153 {10}			1155 {11}
a_1	1182	1182 {6}	1187 {7}	1178 {52}	1173 {8}	1178 {11}
b_2	1272		1272 {6}	1216 {24}	1265 {20}	1267 {7}
b_2	1445	1432 {4}	1438 {6}	1432 {8}	1435 {4}	1438 {6}
a_1	1480		1467 {11}	1468 {13}	1468 {10}	
a_1	1582	1582 {23}	1579 {24}	1559 {84}	1569 {60}	1570 {81}

[a] Band assignments from ref 22.

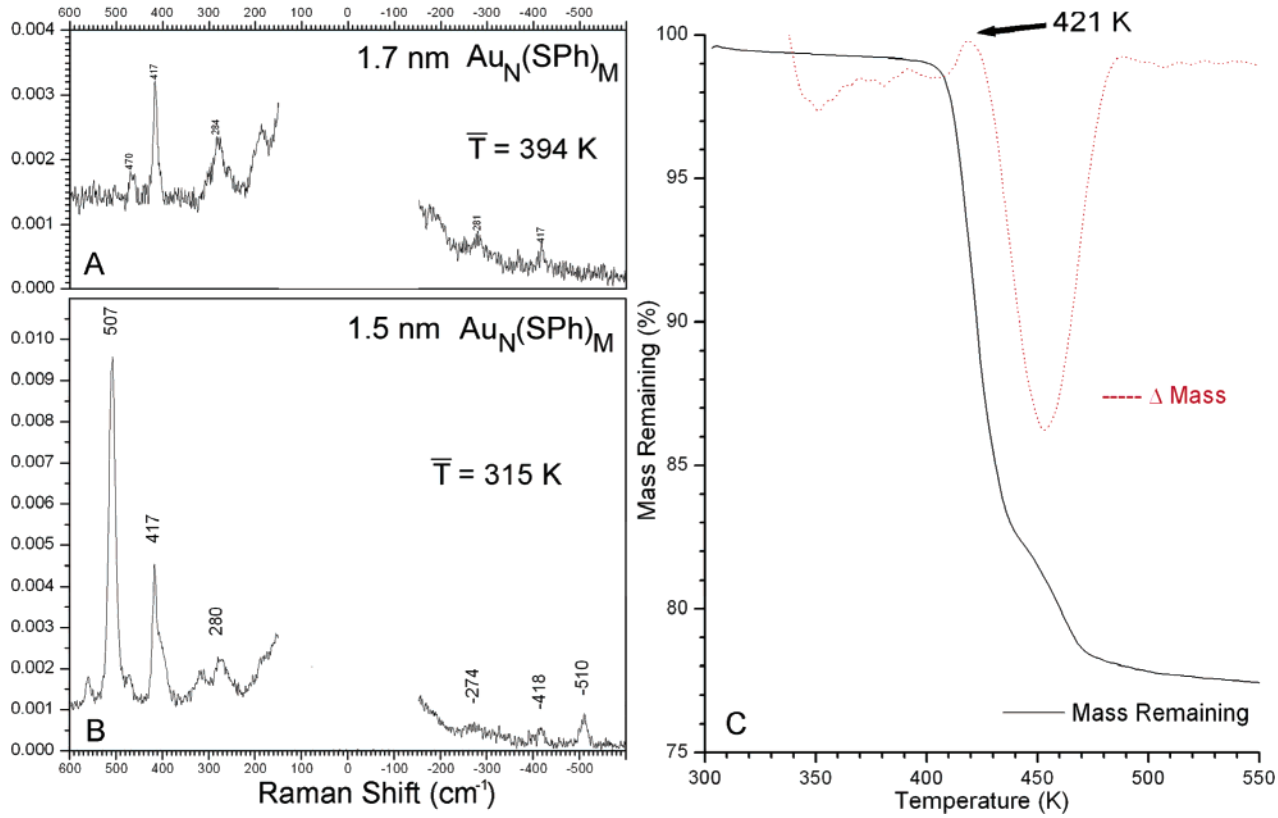

Figure 2. (A) Anti-Stokes and Stokes regions of Raman spectrum for 1.7-nm $Au_N(SPh)_M$. (B) Anti-Stokes and Stokes regions of Raman spectrum for 1.5-nm $Au_N(SPh)_M$. (C) Mass loss vs temperature (black) and its derivative (red) to show the onset of significant mass loss for the 1.7-nm core $Au_N(SPh)_M$ MPCs. Thermogravimetric analysis was performed from 303 to 873 K at a heating rate of 10 K/minute.

binding modes each accounting for 7 benzenethiolates. The spectral assignments for the ortho, meta, and para chemical shifts of the 1.1-nm MPCs were determined by ^{1}H−COSY, shown in the Supporting Information. The shared ^{1}H NMR spectral features of diphenyl disulfide and the 1.5-nm $Au_x(SPh)_y$ MPCs are also evident from the comparative spectra of Figure 3. The chemical shifts of the dominant binding mode of the 1.1-nm MPCs compare favorably with benzenethiolate on 2.16−3.84-nm-diameter cadmium sulfide quantum dots, although the para hydrogen atom is shifted 0.27 ppm upfield on the gold clusters, as indicated in Figure 3.[24] Benzenethiolates are predominantly bound in bridging sites between 2 Cd^{2+} within the crystallographically characterized $Cd_{32}S_{14}(SPh)_{36}$ quantum dot of 1.5-nm core daimeter.[25] This type of binding is similar to that in the $(Au/SPh)_x$ polymer[26] or low coordination number surface bound Au^{I}SR species.[27] Either type of binding places benzenethiolate proximal to an oxidized gold moiety and could produce the observed ^{1}H NMR chemical shifts. The $(Au^ISPh)_x$ polymer was completely insoluble our hands, preventing its characterization by high-resolution ^{1}H NMR for direct comparison with the $Au_x(SPh)_y$ MPCs.

Despite our inability to directly compare $Au_x(SPh)_y$ MPCs with the $(Au^ISPh)_x$ polymer by additional spectroscopic techniques and fully verify its presence, there are several recent

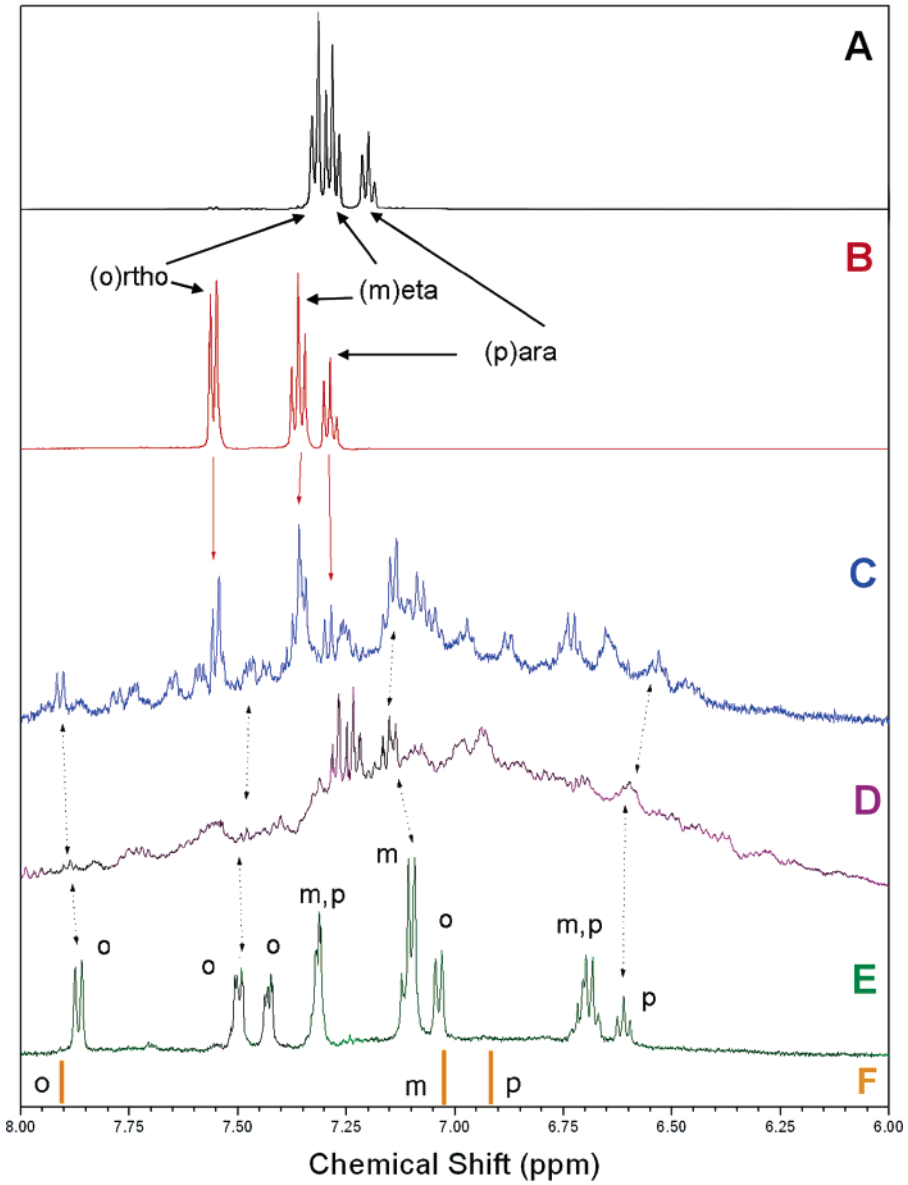

Figure 3. ^{1}H NMR aromatic region spectra of $Au_x(SPh)_y$ MPCs with reference materials. The materials shown from top to bottom are as follows: (A) benzenethiol; (B) diphenyl disulfide; (C) 1.5-nm ~$[Au_{110}(SPh)_{62}]^{6-}$; (D) 1.7-nm ~$[Au_{140}(SPh)_{78}]^{2-}$; (E) 1.1-nm $[Au_{44}(SPh)_{28}]^{2-}$; and (F) chemical shifts of benzenethiolate on CdS quantum dots from ref 24. Dashed black lines indicate the shared dominant spectral features of the MPCs. The red arrows show similar spectral features of diphenyl disulfide and the 1.5 nm ~$[Au_{110}(SPh)_{78}]^{6-}$ clusters. It is also interesting to note that pure benzenethiol does not closely resemble *any* of the $Au_x(SPh)_y$ MPCs. O, M, and P hydrogens are labeled where possible.

experiments suggesting the surface of small gold MPCs are not a bulk fcc gold surface with thiolates bound in 3-fold hollow sites. Direct measurements of methylthiolate monolayers on Au(111) by both photoelectron diffraction and X-ray standing wave analysis indicate that each thiolate sulfur atom is bound to only one gold atom, rather than three, with a proposed reconstruction of the bulk gold surface.[13e,f] Theoretical investigations of methylthiolate on bulk Au(111) by Hammer et al. indicate favored binding in bridging (bidentate) or atop (monodentate) sites on a reconstructed gold surface forming honeycomb or inverted honeycomb gold−thiolate surface layers.[13a,b] Analogous silver−thiolate honeycomb structures resulting from surface reconstruction of methylthiolate chemisorbed onto bulk Ag(111) possessing a $(\sqrt{7} \times \sqrt{7})R19°$ surface phase have been experimentally observed very recently.[13h] Letardi and Cleri have applied ab initio density functional theory to find that the most energetically favorable confirmations are either monodentate (atop) or bidentate (bridging) for benzenethiolate interacting with a three-atom gold cluster.[13c] This theoretical result is consistent with the monodentate binding of aromatic 4-mercaptopyridine (HSC_5H_5N) within the structurally characterized undecagold nanocluster $[Au_{11}(SC_5H_5N)_3(PPh)_7]$.[27] It is vital to note that this cluster lacks bulk fcc gold structure, precluding a direct comparison with theoretical results for thiolates on bulk gold.

Conclusions

Benzenethiolate on the surface of ~1.7-nm gold MPCs provides Raman spectra very similar to $(Au^{(I)}SPh)_x$ polymers, with disulfide-like surface states observed by Raman and ^{1}H NMR spectroscopy within ~1.5-nm core diameter MPCs. The relative enhancements of certain vibrational modes observed for benzenethiolate on roughened gold also resemble those of the $(Au^{(I)}SPh)_x$ polymer. Our results suggest polymeric or oligiomeric Au/thiolate species may be present on the surface of ~1.7-nm gold MPCs with some diphenyl disulfide type

surface species present at diameters of 1.5 nm and below. Our main result is the striking similarities among the Raman spectra of the three Au/SPh phases (clusters, roughened surfaces, polymers) as distinct from the molecular substances (PhSH, NaSPh, PhS−SPh). The simplest explanation for these similarities would be a cross-contamination of the samples by one of the phases responsible for all the observed Raman spectral intensity or a laser decomposition amounting to the same effect. However, the care taken in the preparation, purification, and irradiation of the samples argues against cross-contamination. The next simplest explanation for the similarities is that all three substances have very similar structure and bonding in the gold−thiolate units. This could be true if oligomeric $Au^{(I)}SPh$ structures were the actual "adsorbates" protecting the (reduced) gold surfaces in both the clusters and the roughened electrode surfaces, but absolute determination of these states within the MPCs remains elusive at this time. The presence of $[Au^{I}SPh]$ monomeric species can also not be ruled out entirely, but these clusters are expected to be ∼66% surface atoms, giving roughly 92, 72, and 28 surface atoms for the 1.7, 1.5, and 1.1 nm MPCs, respectively. Comparing the surface gold atoms with surface thiolates previously determined[4] gives coordination numbers of 1.0 to 1.2 for each cluster, values very near the 1:1 ratio of a $(Au^{I}SR)_x$ polymer surface, which may not be coincidental given the spectral similarities presented in this work.

Very recently, Häkkinen et al. used ab initio computations to discover enhanced stability in structures of this type, whereby a core Au_{14} cluster is protected by six ring-type $(AuSR)_4$ adsorbates.[28a,b] The calculation of the Raman spectra of such structures would be most interesting. It is clear that further experimental and theoretical research along these lines will be needed to definitively resolve such questions. Vibrational spectroscopy, including Raman spectroscopy extended into the valuable 50- to 200-cm^{-1} range has an important role to play in elucidating the surface bonding on monolayer protected clusters. If sufficiently crystalline samples lacking TOA or possessing a suitably crystalline cation can be generated, total structural determination may be possible, thereby finally resolving the nature of the gold−thiolate bond in $Au_x(SR)_y$ MPCs.

Acknowledgment. This work was partially supported by the Department of Energy, Office of Basic Energy Sciences under contract no. DE-FG02-02ER45956. We would also like to thank Ruth Liqun Wang. We are most grateful to Matt Foote and Dr. Tim Hanks of Furman University for their ongoing work with lower-energy Raman spectroscopy of these materials.

Supporting Information Available: FT-IR spectra**,** full Raman spectra for the MPCs and $Au^{(I)}SPh$ from 4000 to 150 cm^{-1}, diagrams of benzenethiol normal modes, molar absorptivity plots for the clusters, and aromatic region 2-D COSY ^1H NMR spectra of $[TOA]_2[Au_{44}(SPh)_{28}]$. This material is available free of charge via the Internet at http://pubs.acs.org.

References and Notes

(1) Ulman, A. *Chem. Rev.* **1996**, *96*, 1533.
(2) Link, S.; El-Sayed, M. *Int. Rev. Phys. Chem.* **2000**, *19* (3), 409.
(3) Kudelski, A. *Vib. Spectrosc.* **2005**, *39* (2), 200.
(4) Price, R.; Whetten, R. *J. Am. Chem. Soc.* **2005**, *127* (40), 13750.
(5) Carron, K.; Hurley, G. *J. Phys. Chem.* **1991**, *95*, 9979.
(6) Garrell, R.; Chadwick, J.; Severance, D.; McDonald, N.; Myles, D. *J. Am. Chem. Soc.* **1995**, *117*, 11563.
(7) Svanfranski, C.; Tanner, W.; Laibinis, P.; Garrell, R. *Langmuir* **1998**, *14*, 3570.
(8) Sawaguchi, T.; Mizutani, F.; Yoshimoto, S.; Taniguchi, I. *Electrochim. Acta* **2000**, *45*, 2861.
(9) Dhirani, A.; Zehner, R.; Hsung, R.; Guyot-Sionnest, P.; Sita, L. *J. Am. Chem. Soc.* **1996**, *118*, 3319.
(10) Tao, Y.; Wu, C.; Eu, J.; Lin, W. *Langmuir* **1997**, *13*, 4018.
(11) Wan, L.; Terashima, M.; Noda, H.; Osawa, M. *J. Phys. Chem. B* **2000**, *104*, 3563.
(12) Shon, Y.; Mazzitelli, C.; Murray, R. *Langmuir* **2001**, *17*, 7735.
(13) (a) Molina, L. M.; Hammer, B. *Chem. Phys. Lett.* **2002**, *360* (3−4), 264. (b) Gottschalck, J.; Hammer, B. *J. Chem. Phys.* **2002**, *116*, 784. (c) Letardi, S.; Cleri, F. *J. Chem. Phys.* **2004**, *120*, 10062. (d) Fischer, D.; Curioni, A.; Andreoni, W. *Langmuir* **2003**, *19*, 3567. (e) Kondoh, H.; Iwasaki, M.; Shimada, T.; Amemiya, K.; Yokoyama, T.; Ohta, T.; Shimomura, M.; Kono, S. *Phys. Rev. Lett.* **2003**, *90*, 066102−1. (f) Roper, M. G.; Skegg, M. P.; Fisher, C. J.; Lee, J. J.; Dhanak, V. R.; Woodruff, D. P.; Jones, R. G. *Chem. Phys. Lett.* **2004**, *389*, 87. (g) Yu, M.; Driver, S. M.; Woodruff, D. P. *Langmuir* **2005**, *21* (16), 7285. (h) Woodruff, D.; Yu, M.; Bovet, N.; Satterley, C.; Lovelock, K.; Jones, R.; Dhanak, V. *J. Phys. Chem. B* **2006**, *110*, 2164.
(14) Guo, R.; Murray, R. *J. Am. Chem. Soc.* **2005**, *127*, 12140.
(15) Li, J.; Li, X.; Zhai, H.; Wang, L. *Science* **2003**, *299*, 864.
(16) Puddephatt, R. *The Chemistry of Gold*; Elsevier Scientific Publishing: Oxford, 1978; p 61.
(17) Foote, M.; Hanks, T. Private communication, 2005.
(18) Gui, J.; Stern, D.; Lu, F.; Zapien, D.; Hubbard, A. *Langmuir* **1991**, *7*, 955.
(19) Uehara, J.; Aramaki, K. *J. Electrochem. Soc.* **1991**, *138*, 3245.
(20) (a) Degen, I.; Rowlands, A. *Spectrochim. Acta* **1991**, *9/10*, 1263. (b) Boyen, H.; Kastle, G.; Wegil, F.; Ziemann, P.; Schmid, G.; Garnier, M.; Oelhafen, P. *Phys. Rev. Lett.* **2001**, *87* (27), 6401.
(21) (a) Bigioni, T.; Whetten, R.; Dag, O. *J. Phys. Chem. B* **2000**, *104*, 6983. (b) Huang, T.; Murray, R. *J. Phys. Chem. B* **2001**, *105*, 12498. (c) Link, S.; Beeby, A.; Fitzgerald, S.; El-Sayed, M.; Schaaff, T.; Whetten, R. *J. Phys. Chem. B* **2002**, *106*, 3410. (d) Lee, D.; Donkers, R.; Wang, G.; Harper, A.; Murray, R. *J. Am. Chem. Soc.* **2004**, *126*, 6193. (e) Negishi, Y.; Takasugi, Y.; Sato, S.; Yao, H.; Kimura, K.; Tsukuda, T. *J. Am. Chem. Soc.* **2004**, *126*, 6518. (f) Negishi, Y.; Nobusada, K.; Tsukuda, T. *J. Am. Chem. Soc.* **2005**, *127*, 5261. (g) Wang, G.; Huang, T.; Murray, R.; Menard, L.; Nuzzo, R. *J. Am. Chem. Soc.* **2005**, *127*, 812.
(22) Varsanyi, G. *Assignments for Vibrational Spectra of Seven Hundred Benzene Derivatives*; John Wiley and Sons: New York, 1974.
(23) (a) Kohlmann, O.; Steinmetz, W.; Mao, X.; Wuelfing, P.; Templeton, A.; Murray, R.; Johnson, C. *J. Phys. Chem. B* **2001**, *105*, 8801. (b) Schaaff, T.; Shafigullin, M.; Khoury, J.; Vezmar, I.; Whetten, R. *J. Phys. Chem. B* **2001**, *105*, 8785. (c) Shon, Y.; Mazzitelli, C.; Murray, R. *Langmuir* **2001**, *17*, 7735. (d) Donkers, R.; Lee, D.; Murray, R. *Langmuir* **2004**, *20*, 1945. (d) Wang, W.; Murray, R. *Langmuir* **2005**, *21*, 7015. (e) Guo, R.; Song, Y.; Wang, G.; Murray, R. *J. Am. Chem. Soc.* **2005**, *127*, 2752.
(24) Sachleben, J.; Colvin, V.; Emsley, L.; Wooten, W.; Alivisatos, P. *J. Phys. Chem. B* **1998**, *102*, 10117.
(25) Herron, N.; Calabrese, J.; Farneth, W.; Wang. Y. *Science* **1993**, *259*, 1426.
(26) Bates, P.; Waters, J. *Acta Crystallogr.* **1985**, *C41*, 862.
(27) Nunokawa, K.; Onaka, S.; Ito, M.; Horibe, M.; Yonezawa, T.; Nishihara, H.; Ozeki, T.; Chiba, H.; Watase, S.; Nakamoto, M. *J. Organomet. Chem.* **2006**, *691*, 638.
(28) (a) Hakkinen, H.; Walter, M.; Gronbeck, H. *J. Phys. Chem. B* **2006**, *110*, 9927. (b) Gronbeck, H.; Walter, M.; Hakkinen, H. *J. Am. Chem. Soc.* **2006**, *128*, 10268.